Three-Dimensional Location Estimation of Circular Features for Machine Vision

Reza Safaee-Rad, Ivo Tchoukanov, *Member, IEEE,* Kenneth Carless Smith, *Fellow, IEEE,* and Bensiyon Benhabib

Abstract— Estimation of 3-D information from 2-D image coordinates is a fundamental problem both in machine vision and computer vision. Circular features are the most common quadratic-curved features that have been addressed for 3-D location estimation. In this paper, a closed-form analytical solution to the problem of 3-D location estimation of circular features is presented. Two different cases are considered: 1) 3-D orientation and 3-D position estimation of a circular feature when its radius is known, and 2) 3-D orientation and 3-D position estimation of a circular feature when its radius is not known. As well, extension of the developed method to 3-D quadratic features is addressed. Specifically, a closed-form analytical solution is derived for 3-D position estimation of spherical features. For experimentation purposes, simulated as well as real setups were employed. Simulated experimental results obtained for all three cases mentioned above verified the analytical method developed in this paper. In the case of real experiments, a set of circles located on a calibration plate, whose locations were known with respect to a reference frame, were used for camera calibration as well as for the application of the developed method. Since various distortion factors had to be compensated in order to obtain accurate estimates of the parameters of the imaged circle—an ellipse—with respect to the camera's image frame, a sequential compensation procedure was applied to the input grey-level image. The experimental results obtained once more showed the validity of the total process involved in the 3-D location estimation of circular features in general and the applicability of the analytical method developed in this paper in particular.

I. INTRODUCTION

ESTIMATION of 3-D information from 2-D image coordinates is a fundamental problem in both machine vision and computer vision. This problem exists in two forms: the direct and the inverse. When the camera parameters (the intrinsic: effective focal length, lens distortion factors, etc., and the extrinsic: 3-D position and 3-D orientation of the camera frame) are given in addition to the 2-D image coordinates, the problem is of the direct type. On the other hand, if

R. Safaee-Rad is with the Computer Integrated Manufacturing Laboratory, Department of Mechanical Engineering, University of Toronto, Toronto, Ont. M5S 1A4, Canada.

I. Tchoukanov is with the Department of Electrical Engineering, University of Toronto, Toronto, Ont. M5S 1A4, Canada.

K. C. Smith is with the Department of Mechanical Engineering, the Department of Electrical Engineering, and the Department of Computer Science, University of Toronto, Toronto, Ont. M5S 1A4, Canada.

B. Benhabib is with the Department of Mechanical Engineering and the Department of Electrical Engineering, University of Toronto, Toronto, Ont. M5S 1A4, Canada.

IEEE Log Number 9202103.

the 3-D coordinates are given in addition to the 2-D image coordinates, the problem is of the inverse type. In the first (direct) type, the objective is to estimate the 3-D location of objects, landmarks, and features. This type of problem occurs in many areas: for example, in automatic assembly, tracking, and industrial metrology. In the second (inverse) type, the objective is to estimate the relevant camera parameters: for a fixed camera, all the intrinsic and extrinsic parameters; for a moving camera, only the extrinsic parameters, namely, its 3-D location. This type of problem occurs in areas such as camera calibration, camera-robot calibration for eye-on-hand systems, and autonomous mobile robot guidance.

The problem of 3-D location estimation of objects in a scene has been addressed extensively in the applied literature where it is referred to as feature-based 3-D location estimation of objects. The body of literature dealing with this general problem is concerned with developing mathematical methods for the estimation of an object's location based on *point* features, whether it is a 3-point problem (also called the triangle-pose problem [1]–[4]), a 4-point problem [1], [5]–[12], or an n-point problem [13]–[17]. Estimation of the object's location based on *line* features, whose mathematics is similar to that of point features, has also been studied [18]–[22]. As well, for *quadratic-curved* features, a general method has been developed [20]. However, this method is iterative and requires an initial estimate.

A circular shape, representing a particular special case of quadratic-curved features, is the most common quadratic that has been addressed for 3-D location estimation, mainly due to the following reasons: 1) many manufactured objects have circular holes or circular surface contours; 2) a circle has the following properties from a mathematical point of view: its perspective projection in any arbitrary orientation is always an exact ellipse, and it can be defined with only three parameters due to its symmetry with respect to its center; 3) a circle has been shown to have the property of high image-location accuracy [23], [24]; and 4) the complete boundary or an arc of a projected circular feature can be used for 3-D location estimation without knowing the exact point correspondence.

As a result of the above-mentioned properties, circular features have been used in various machine-vision-related problems. For example, they have been used for accurate estimation of a mobile robot's position using circular landmarks [25]–[29], for recognition (identification and 3-D location estimation) of 3-D premarked objects using circular markers [30], [31], for feature estimation of 3-D objects using a tapered light beam [32], for 3-D orientation estimation of objects with

circular surface contours [33], for objects that have holes [34] and for cylindrical objects marked by two circular stripes that are placed radially around them [35], and for reconstruction of the 3-D structure and motion of a scene undergoing relative rotational motion with respect to the camera [36].

For 3-D location estimation based on circular features, approximate and exact solution methods have been proposed. In the approximate-solution methods [25]–[29], three difficulties remain in the mathematical solutions presented. The first concerns a set of simplifying assumptions made in order to reduce a complex 3-D problem to a simple 2-D problem, yet assumptions that lead to further complications. For example, researchers assume that the optical axis of the camera passes through the center of the circular feature and/or assume orthogonal projection instead of perspective projection. The second difficulty is evidence of an incorrect claim regarding the actual effect of perspective projection on the image of a circle, an ellipse, which states that the perspective projection of a circle is not an exact ellipse but, rather, a distorted one. The third difficulty is that, in general, authors do not discuss the error introduced by each approximation. A detailed analysis of the common approximate solutions are presented elsewhere [37].

There have been several methods proposed to solve the circular-feature-based 3-D location estimation of objects (which we call the circular-feature problem in this paper) in a scene under general conditions without simplifying assumptions. An iterative method has been addressed in [38]. Closed-form solutions for the circular-feature problem have also been developed based on linear algebra [36], [39], but these methods are mathematically complex and, being algebra-based, do not provide a geometrical representation of the problem nor a geometrical interpretation of the resulting solutions.

Recently, a closed-form mathematical solution, based on 3-D analytical geometry of circular and spherical features, was published [40]. This solution method has several advantages: it is a closed-form solution, it gives only the necessary number of solutions (with no redundant solutions), and it uses simple mathematics involving 3-D analytic geometry.

We have previously addressed the circular-feature problem under the assumption that the optical axis of the camera is coplanar with the surface normal of the circular feature, and have derived a closed-form solution based on simple geometrical reasoning [31]. Also, we have derived another closed-form mathematical solution to the general form of the circular-feature problem based on 3-D analytical geometry [41]. The complete solution of this problem is presented in this paper. This closed-form solution provides all the above-mentioned advantages compared to all previous methods. But, as well, it has the following additional advantages: 1) it is based on simple mathematics, 2) it provides solutions for the case in which there does not exist *a priori* knowledge concerning the radius of the marker, 3) it can be extended and applied to general quadratic surfaces due to its more general formulation, and 4) it provides both geometrical representation of the problem and geometrical interpretation of the resulting solutions.

In Section II of this paper, the analytical formulation of the problem is presented, which is based on decomposition of the 3-D location problem into a 3-D orientation and a 3-D position estimation problem. In Section III, the proposed analytical solution method is presented: To derive a closed-form analytical solution method for the 3-D orientation problem, we utilize an analytical method for reduction of the general equation of 3-D quadratic surfaces to its central form (Section III-A). For the 3-D position estimation problem, two cases are addressed: when the feature's radius is known and when it is not known (Section III-B). Extension of the developed method to 3-D quadratic features (as opposed to 2-D features) is addressed in Section IV, wherein, a closed-form analytical solution method specifically for spherical features is derived. Experimental results are presented in Section V, where simulated as well as real setups are employed. Simulated experimental results are obtained for three different cases (Section V-A): 1) 3-D orientation and 3-D position estimation of a circular feature when its radius is known; 2) 3-D position and 3-D orientation estimation of a circular feature when its radius is *not* known; and 2) 3-D position estimation of a spherical feature. For a real-case setup, the method developed has been applied to a set of circles located on a calibration plate (Section V-B) for 3-D orientation and 3-D position estimation purposes. Conclusions are presented in Section VI.

II. ANALYTICAL FORMULATION OF THE PROBLEM

The analytical method proposed in this paper is based on the decomposition of the 3-D location estimation problem into two parts: first, the 3-D orientation (the surface normal) of the circular feature is estimated; subsequently, based on the estimated orientation, the 3-D position of the feature is calculated. The analytical formulation of the 3-D orientation problem is presented in this section.

Given the effective focal length of a camera, and the five basic parameters of an ellipse in the image-coordinate frame (embodying the perspective projection of a circular feature in 3-D object space onto a 2-D image space [37]), it is required to estimate the circular-feature's 3-D orientation with respect to the camera frame.

This problem is equivalent to the following: Given a 3-D cone surface defined by a base (the perspective projection of a circular feature in the image plane) and a vertex (the center of the camera's lens) with respect to a reference frame, determine the orientation of a plane (with respect to the same reference frame) that intersects the cone and generates a circular curve.

The equation of the cone whose vertex is the point (α, β, γ) and whose base is defined by the ellipse

$$F(x,y) \equiv a'x^2 + 2h'xy + b'y^2 + 2g'x + 2f'y + d' = 0$$
$$z = 0 \tag{1}$$

can be expressed as [42]:

$$z^2 F(\alpha, \beta) - z\gamma \left(x\frac{\partial F}{\partial x} + y\frac{\partial F}{\partial y} + t\frac{\partial F}{\partial t} \right) + \gamma^2 F(x,y) = 0 \tag{2}$$

where

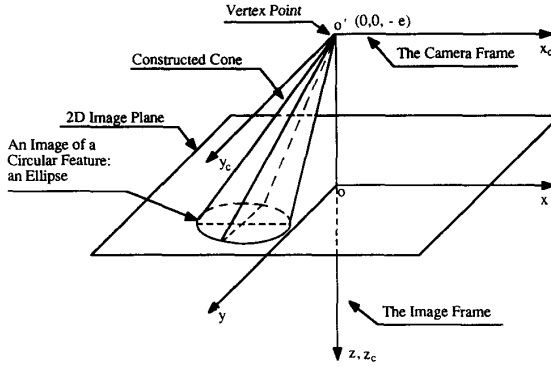$$F(x,y,t) = a'x^2 + 2h'xy + b'y^2 + 2g'xt + 2f'yt + d't^2 = 0.$$

Fig. 1.   Schematic representation of the problem for a circular feature.

In (2), t is an auxiliary variable by which $F(x, y)$ is made homogeneous $(F(x, y, t))$. The terms $(\partial F / \partial x)$ and $(\partial F / \partial y)$ are evaluated at $x = \alpha$ and $y = \beta$. As well, the term $t(\partial F / \partial t)$ is calculated by first taking the derivative of the homogeneous equation with respect to t and then evaluating it at $x = \alpha$, $y = \beta$, and $t = 1$. The general form of the equation of a cone derived using the above equation is as follows (with respect to the *image* frame):

$$ax^2 + by^2 + cz^2 + 2fyz + 2gzx + 2hxy + 2ux + 2vy + 2wz + d = 0 \tag{3}$$

where

$$a = \gamma^2 a'$$
$$b = \gamma^2 b'$$
$$c = a'\alpha^2 + 2h'\alpha\beta + b'\beta^2 + 2g'\alpha + 2f'\beta + d'$$
$$d = \gamma^2 d'$$
$$f = -\gamma(b'\beta + h'\alpha + f')$$
$$g = -\gamma(h'\beta + a'\alpha + g')$$
$$h = \gamma^2 h'$$
$$u = \gamma^2 g'$$
$$v = \gamma^2 f'$$
$$w = -\gamma(f'\beta + g'\alpha + d').$$

The constructed 3-D cone surface is shown schematically in Fig. 1 for $\alpha = 0$, $\beta = 0$, and $\gamma = -e$, where e is the effective focal length of the camera.

It can be proven [43] that all parallel planar sections of a conicoid are similar and similarly situated conics. Thus, an intersection plane can be defined by $lx + my + nz = 0$. Therefore, the problem of finding the coefficients of the equation of a plane for which the intersection is circular can be expressed mathematically as finding l, m, and n such that the intersection of the conical surface (3) with the following surface is a circle:

$$lx + my + nz = 0 \tag{4}$$

where $l^2 + m^2 + n^2 = 1$. Having found the coefficients of the equation of the plane, the direction numbers (l', m', n') of the orientation of the circular feature can be estimated from

$$\frac{l}{l'} = \frac{m}{m'} = \frac{n}{n'}. \tag{5}$$

III. An Analytical Solution of the Problem

The solution of the 3-D orientation problem in its general form leads to a set of two highly nonlinear equations, whose solutions would require numerical methods (see Appendix A). Furthermore, this process would produce at least eight sets of solutions, though there exist, at most, two acceptable sets of solutions. In the following section, an alternative analytical solution method is presented, based on a reduction of the general equation of conicoids.

A. 3-D Orientation Estimation of a Circular Feature

1) Reduction of the General Equation of Conicoids: The first step in the proposed analytical solution to the circular-feature-orientation estimation problem is to reduce the general equation of conicoids (3) to a more compact form [43]

$$\lambda_1 X^2 + \lambda_2 Y^2 + \lambda_3 Z^2 = \mu \tag{6}$$

where the XYZ frame is called the canonical frame of conicoids. It will be shown (in Section III-A-2) that the reduction of the general equation of a cone to the above form (6) will result in a closed-form analytical solution. In essence, this reduction is based on a transformation consisting first of a rotation and then a translation of the xyz frame to the canonical XYZ frame.

Let the homogeneous equation of conicoids be defined as

$$ax^2 + by^2 + cz^2 + 2fyz + 2gzx + 2hxy = 0. \tag{7}$$

The problem is to find the elements of a rotational transformation (T_1)

$$\begin{bmatrix} x \\ y \\ z \\ 1 \end{bmatrix} = \begin{bmatrix} l_1 & l_2 & l_3 & 0 \\ m_1 & m_2 & m_3 & 0 \\ n_1 & n_2 & n_3 & 0 \\ 0 & 0 & 0 & 1 \end{bmatrix} \begin{bmatrix} x' \\ y' \\ z' \\ 1 \end{bmatrix} \tag{8}$$

such that (7) reduces to the following form:

$$\lambda_1 x'^2 + \lambda_2 y'^2 + \lambda_3 z'^2 = \mu. \tag{9}$$

It has been proven in [43] that if λ_1, λ_2, and λ_3 are the roots of the following equation (called the discriminating cubic)

$$\lambda^3 - \lambda^2(a + b + c) + \lambda(bc + ca + ab - f^2 - g^2 - h^2)$$
$$- (abc + 2fgh - af^2 - bg^2 - ch^2) = 0 \tag{10}$$

then the elements of the rotational transformation would be obtained from the following equations:

$$\frac{al_i + hm_i + gn_i}{l_i} = \frac{hl_i + bm_i + fn_i}{m_i}$$
$$= \frac{gl_i + fm_i + cn_i}{n_i} = \lambda_i, \quad i = 1, 2, 3. \tag{11}$$

From (11) the following explicit relations are derived:

$$m_i = 1 / \sqrt{1 + (t_1/t_2)^2 + t_3^2}$$
$$l_i = (t_1/t_2)m_i$$
$$n_i = t_3 m_i \tag{12}$$

where

$$t_1 = (b - \lambda_i)g - fh$$
$$t_2 = (a - \lambda_i)f - gh$$
$$t_3 = -(a - \lambda_i)(t_1/t_2)/g - h/g.$$

The estimated values for l_i, m_i, and n_i must satisfy the right-hand rule.

If (7) is expressed in the following matrix form: $X^t A X = 0$, where X^t is a row matrix $[xyz]$, then by applying the general method of diagonalization of quadratic forms [44], equivalent results can be obtained. That is, the column vectors of the rotational transformation (8) are the eigenvectors of matrix A, and its eigenvalues correspond to the coefficients of (6).

Through the rotational transformation (8), the general equation of conicoids (3) would reduce to the following form:

$$\lambda_1 x'^2 + \lambda_2 y'^2 + \lambda_3 z'^2 + 2(ul_1 + vm_1 + wn_1)x' +$$
$$2(ul_2 + vm_2 + wn_2)y' + 2(ul_3 + vm_3 + wn_3)z' + d = 0. \tag{13}$$

To reduce (13) to (6), the following translational transformation (T_2) is applied:

$$\begin{bmatrix} x' \\ y' \\ z' \\ 1 \end{bmatrix} = \begin{bmatrix} 1 & 0 & 0 & -(ul_1 + vm_1 + wn_1)/\lambda_1 \\ 0 & 1 & 0 & -(ul_2 + vm_2 + wn_2)/\lambda_2 \\ 0 & 0 & 1 & -(ul_3 + vm_3 + wn_3)/\lambda_3 \\ 0 & 0 & 0 & 1 \end{bmatrix} \begin{bmatrix} X \\ Y \\ Z \\ 1 \end{bmatrix}. \tag{14}$$

The set of equations obtained when the two transformations are combined is

$$\begin{bmatrix} x \\ y \\ z \\ 1 \end{bmatrix} = \begin{bmatrix} l_1 & l_2 & l_3 & -(ul_1 + vm_1 + wn_1)/\lambda_1 \\ m_1 & m_2 & m_3 & -(ul_2 + vm_2 + wn_2)/\lambda_2 \\ n_1 & n_2 & n_3 & -(ul_3 + vm_3 + wn_3)/\lambda_3 \\ 0 & 0 & 0 & 1 \end{bmatrix} \begin{bmatrix} X \\ Y \\ Z \\ 1 \end{bmatrix}. \tag{15}$$

Thus, through the general transformation (15), the general equation of conicoids (3) would reduce to what is referred to as the equation of central conicoids (6).

If the general transformation (15) is applied to the general equation of a *cone*, it has been proven [42] that its equation would be in the form of (6), where $\mu = 0$ and two of the three coefficients would be always positive with one always negative. If positive values are assigned to λ_1 and λ_2, and a negative value to λ_3, then the principal axis of the central cone would be the Z axis of the XYZ frame. This case is shown in Fig. 2. The intersections of parallel planes $Z = k$ with the central cone would generally be ellipses of different sizes

$$\frac{X^2}{(k\sqrt{(-\lambda_3/\lambda_1)})^2} + \frac{Y^2}{(k\sqrt{(-\lambda_3/\lambda_2)})^2} = 1. \tag{16}$$

The major and minor radii of the ellipse (16) are functions of four parameters: $\lambda_1, \lambda_2, \lambda_3$, and k. Parameter k is a function
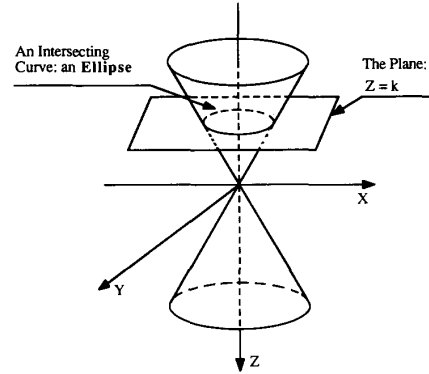

Fig. 2. The central form of a cone: an *elliptical* right cone.

of the radius of the circular feature. The other three parameters are functions of the parameters of the base of the constructed cone (1) and the 3-D coordinates of the center of the camera's lens (α, β, γ); refer to (10) and (3).

2) Circular Section of a Central Cone: In this section, the 3-D orientation problem will be solved analytically by considering the equation of a cone in its central form. Thus, it is required to find the coefficients of the equation of a particular plane (with respect to the XYZ frame)

$$lX + mY + nZ = p \tag{17}$$

whose intersection with a central cone (for which it is assumed that the first two coefficients are positive and the third one is negative)

$$\lambda_1 X^2 + \lambda_2 Y^2 + \lambda_3 Z^2 = 0 \tag{18}$$

would be a circle.

In order to find the equation of the intersection curve of the above two surfaces, the following rotational transformation (T_3) can be used:

$$\begin{bmatrix} X \\ Y \\ Z \\ 1 \end{bmatrix} = \begin{bmatrix} \frac{-m}{\sqrt{l^2+m^2}} & -\frac{ln}{\sqrt{l^2+m^2}} & l & 0 \\ \frac{l}{\sqrt{l^2+m^2}} & -\frac{mn}{\sqrt{l^2+m^2}} & m & 0 \\ 0 & \sqrt{l^2 + m^2} & n & 0 \\ 0 & 0 & 0 & 1 \end{bmatrix} \begin{bmatrix} X' \\ Y' \\ Z' \\ 1 \end{bmatrix}. \tag{19}$$

This transformation is defined such that the new Z axis (i.e., Z') would be normal to the plane $lX + mY + nZ = P$. Applying the above rotational transformation, the equation of the plane would be of the form $Z' = p$; thus, the equation of the intersecting curve would be of the following form:

$$\left[\frac{\lambda_1 m^2}{l^2 + m^2} + \frac{\lambda_2 l^2}{l^2 + m^2}\right] X'^2 + \left[\frac{\lambda_1 l^2 n^2}{l^2 + m^2} + \frac{\lambda_2 m^2 n^2}{l^2 + m^2} + \lambda_3 (l^2 + m^2)\right] Y'^2 + \left[\frac{2\lambda_1 lmn}{l^2 + m^2} - \frac{2\lambda_2 lmn}{l^2 + m^2}\right] X'Y'$$
$$+ p\left[-\frac{2\lambda_1 lm}{\sqrt{l^2 + m^2}} + \frac{2\lambda_2 lm}{\sqrt{l^2 + m^2}}\right] X' + p\left[-\frac{2\lambda_1 l^2 n}{\sqrt{l^2 + m^2}} - \frac{2\lambda_2 m^2 n}{\sqrt{l^2 + m^2}} + 2\lambda_3 n\sqrt{l^2 + m^2}\right] Y' + p^2[\lambda_1 l^2 + \lambda_2 m^2 + \lambda_3 n^2] = 0. \tag{20}$$

On the other hand, the necessary and sufficient conditions for which a general quadratic equation of the form

$$Ax^2 + Bxy + Cy^2 + Dx + Ey + F = 0 \qquad (21)$$

represents a circle would be

$$A = C, \quad B = 0. \qquad (22)$$

Thus, for (20), the following two conditions must exist:

$$2(\lambda_1 - \lambda_2)\frac{lmn}{l^2 + m^2} = 0 \qquad (23)$$

$$\frac{1}{l^2 + m^2}(\lambda_1 m^2 + \lambda_2 l^2) = \frac{\lambda_1 l^2 n^2}{l^2 + m^2} + \frac{\lambda_2 m^2 n^2}{l^2 + m^2} + \lambda_3(l^2 + m^2). \qquad (24)$$

Knowing that $l^2 + m^2 \neq 0$ (except for the special case of a right circular cone, that is, for case IV below), (24) is simplified as

$$(\lambda_1 l^2 + \lambda_2 m^2)n^2 + \lambda_3(l^2 + m^2)^2 = \lambda_1 m^2 + \lambda_2 l^2. \qquad (25)$$

Furthermore, the general relationship between coefficients exists:

$$l^2 + m^2 + n^2 = 1. \qquad (26)$$

Thus, there are three equations ((23), (25), and (26)) and three unknowns l, m, and n.

Considering (23), four possible cases exist.

Case I—$l = 0$: Based on (23), (25), and (26), the following solutions are derived:

$$n = \pm\sqrt{\frac{\lambda_1 - \lambda_3}{\lambda_2 - \lambda_3}}$$

$$m = \pm\sqrt{\frac{\lambda_2 - \lambda_1}{\lambda_2 - \lambda_3}}$$

$$l = 0. \qquad (27)$$

The above solutions must be checked to determine whether they are acceptable. If it is assumed that the principal axis of the central cone is the Z axis, then

$$\lambda_1 > 0, \quad \lambda_2 > 0, \quad \lambda_3 < 0 \qquad (28)$$

which leads to the following inequalities:

$$\lambda_1 - \lambda_3 > 0, \quad \lambda_2 - \lambda_3 > 0. \qquad (29)$$

Based on these inequalities, one can check the solutions. The solutions for n are acceptable since the expression $(\lambda_1 - \lambda_3)/(\lambda_2 - \lambda_3)$ is positive. The solution for m would be acceptable if $\lambda_2 > \lambda_1$.

If it is assumed that $\lambda_2 > \lambda_1$, then there exist four solutions to the problem. But these are four symmetrical solutions with respect to the origin of XYZ frame and consequently represent only two unique solutions. If one takes the solutions on the positive section of Z axis, then the two solutions would be

$$n = +\sqrt{\frac{\lambda_1 - \lambda_3}{\lambda_2 - \lambda_3}}$$

$$m = \pm\sqrt{\frac{\lambda_2 - \lambda_1}{\lambda_2 - \lambda_3}}$$

$$l = 0. \qquad (30)$$

Case II—$m = 0$: Following the same arguments for case I, two solutions can be derived that would be acceptable only if $\lambda_1 > \lambda_2$:

$$n = +\sqrt{\frac{\lambda_2 - \lambda_3}{\lambda_1 - \lambda_3}}$$

$$m = 0$$

$$l = \pm\sqrt{\frac{\lambda_1 - \lambda_2}{\lambda_1 - \lambda_3}}. \qquad (31)$$

Case III—$n = 0$: In this case, the following solutions for l and m are derived:

$$l = \pm\sqrt{\frac{\lambda_3 - \lambda_1}{\lambda_2 - \lambda_1}}$$

$$m = \pm\sqrt{\frac{\lambda_2 - \lambda_3}{\lambda_2 - \lambda_1}}. \qquad (32)$$

However, for the solutions of l to be acceptable, one must have $\lambda_2 < \lambda_1$. For the solutions of m to be acceptable, on the other hand, one must have $\lambda_2 > \lambda_1$. Thus, it can be claimed that an acceptable solution does not exist for this case.

Case IV—$\lambda_1 = \lambda_2$: This is a special case, since it imposes a constraint on the coefficients of the equation of a central cone. In this case, the equation of the central cone represents a right circular cone (which implies that the central surface normal of the circular feature passes through the origin of the camera frame), and thus, any plane $Z = k$ intersects it and generates a circular intersection curve. Thus, there exists only one solution:

$$n = 1$$

$$m = 0$$

$$l = 0. \qquad (33)$$

In conclusion, one can state that, generally, there exist two acceptable solutions to the problem. Under special conditions, these two solutions reduce to a single solution. Once the coefficients of the equation of the desired plane have been estimated, the direction cosines of the surface normal of the circular feature can be estimated using (5).

3) The Computation Procedure for Surface-Normal Estimation: The computation procedure for the proposed analytical method for surface-normal estimation of a circular feature consists of the following steps:

Step 1—Estimation of the coefficients of the general equation of the cone: Estimate the coefficients a, b, c, f, g, h, u, v, w, and d as defined in (3), based on knowledge of the coefficients of the equation of the ellipse — the image of the circular feature — (in the image-coordinate frame) and the effective focal length of the camera.

Step 2—Reduction of the equation of the cone: Determine the coefficients λ_1, λ_2, and λ_3 in (18), by solving the discriminating cubic equation (10), such that λ_1 and λ_2 are positive.

Step 3—Estimation of the coefficients of the equation of the circular-feature plane: Having estimated the coefficients of the central cone in step 2 (λ_i in (18)), three possible cases occur: 1) $\lambda_1 < \lambda_2$, for which the solutions would be (30); 2) $\lambda_1 > \lambda_2$, for which the solutions would be (31); and 3) $\lambda_1 = \lambda_2$, for which the solutions would be (33).

Step 4—Estimation of the direction cosines of the surface normal with respect to the camera frame: Since only the orientation of the circular feature is needed, one must consider only the rotational transformation involved in this method. Thus, first, estimate the elements of the rotational transformation between the $x'y'z'$ frame and the xyz frame (see (8)) by using (12); then the coefficients of the equation of the desired plane with respect to the camera xyz frame can be estimated by applying this rotational transformation. Following which, the direction cosines of the surface normal are estimated using (5).

A numerical example for the above computation procedure is given in Section V-A-1.

B. 3-D Position Estimation of a Circular Feature

The position of a circle is defined by its center coordinates (x_{co}, y_{co}, z_{co}) with respect to the $x_c y_c z_c$ *camera* frame. It is noted that the transformation between the image frame (xyz) and the camera frame (T_o) is defined as follows:

$$\begin{bmatrix} x_c \\ y_c \\ z_c \\ 1 \end{bmatrix} = \begin{bmatrix} 1 & 0 & 0 & 0 \\ 0 & 1 & 0 & 0 \\ 0 & 0 & 1 & +e \\ 0 & 0 & 0 & 1 \end{bmatrix} \begin{bmatrix} x \\ y \\ z \\ 1 \end{bmatrix} \quad (34)$$

where e is the effective focal length of the camera. Depending on whether the radius of the circle is known or not known, two different methods can be applied.

Case I—Radius is known: The radius of the circular feature might be known. That is, either it is prespecified or it has been estimated through other sensory system. In this case, based on the knowledge of the orientation of a circle and its radius, one can solve the position problem as follows. The problem is simplified by first solving it in the $X'Y'Z'$ frame and then applying the total transformation, $T = T_o T_1 T_2 T_3$ where

$$X'Y'Z' \xrightarrow{\text{Rotation}}_{T_3} > XYZ \xrightarrow{\text{Translation}}_{T_2}$$
$$> x'y'z' \xrightarrow{\text{Rotation}}_{T_1} > xyz \xrightarrow{\text{Translation}}_{T_o} > x_c y_c z_c \quad (35)$$

to estimate the position with respect to the camera frame $(x_c y_c z_c)$. This is possible only because the radius of a circular feature is invariant with respect to the rotational and translational transformations of a frame.

The desired plane of intersection is defined as $Z' = p$ with respect to the $X'Y'Z'$ frame. The elements of the transformation (19) are already known (since the coefficients of the equation of the desired plane l, m, n are known through application of the above-mentioned computation procedure in Section III-A-3). Thus, if one defines the transformation as

$$\begin{bmatrix} X \\ Y \\ Z \\ 1 \end{bmatrix} = \begin{bmatrix} l_1 & m_1 & n_1 & 0 \\ l_2 & m_2 & n_2 & 0 \\ l_3 & m_3 & n_3 & 0 \\ 0 & 0 & 0 & 1 \end{bmatrix} \begin{bmatrix} X' \\ Y' \\ Z' \\ 1 \end{bmatrix} \quad (36)$$

then the equation of the circle with respect to the $X'Y'Z'$

frame (20) would be $(Z' = p)$

$$(\lambda_1 l_1^2 + \lambda_2 l_2^2 + \lambda_3 l_3^2) X'^2 + (\lambda_1 m_1^2 + \lambda_2 m_2^2 + \lambda_3 m_3^2) Y'^2$$
$$+ 2(\lambda_1 l_1 m_1 + \lambda_2 l_2 m_2 + \lambda_3 l_3 m_3) X'Y'$$
$$+ 2p(\lambda_1 l_1 n_1 + \lambda_2 l_2 n_2 + \lambda_3 l_3 n_3) X'$$
$$+ 2p(\lambda_1 m_1 n_1 + \lambda_2 m_2 n_2 + \lambda_3 m_3 n_3) Y'$$
$$+ p^2(\lambda_1 n_1^2 + \lambda_2 n_2^2 + \lambda_3 n_3^2) = 0. \quad (37)$$

As was noted earlier (see (21) and (22)), the coefficient of the $X'Y'$ term must be zero and the coefficients of X'^2 and Y'^2 must be equal. Now, if

$$A \equiv (\lambda_1 l_1^2 + \lambda_2 l_2^2 + \lambda_3 l_3^2)$$
$$B \equiv (\lambda_1 l_1 n_1 + \lambda_2 l_2 n_2 + \lambda_3 l_3 n_3)$$
$$C \equiv (\lambda_1 m_1 n_1 + \lambda_2 m_2 n_2 + \lambda_3 m_3 n_3)$$
$$D \equiv (\lambda_1 n_1^2 + \lambda_2 n_2^2 + \lambda_3 n_3^2) \quad (38)$$

then the equation of the circle would become (in its standard form)

$$\left(X' + \frac{pB}{A}\right)^2 + \left(Y' + \frac{pC}{A}\right)^2 = \frac{p^2 B^2}{A^2} + \frac{p^2 C^2}{A^2} - \frac{p^2 D}{A}. \quad (39)$$

However, the radius (r) is known, and, therefore, one can estimate the value of the parameter p from the following equation:

$$p = \pm \frac{Ar}{\sqrt{B^2 + C^2 - AD}}. \quad (40)$$

As can be seen, there exist two solutions, one negative and one positive: one on the positive z axis and one on the negative z axis. Since only the positive one is acceptable in our case (being located in front of the camera), the coordinates of the center of the circle with respect to the $X'Y'Z'$ frame are

$$X_o' = -\frac{B}{A} Z_o'$$
$$Y_o' = -\frac{C}{A} Z_o'$$
$$Z_o' = \pm \frac{Ar}{\sqrt{B^2 + C^2 - AD}} \quad (41)$$

under the condition that the sign of the coordinate Z_o' is selected such that the coordinate z_{co} in the $x_c y_c z_c$ frame would be positive.

To estimate the coordinates of the circle's center with respect to the $x_c y_c z_c$ frame (the *camera* frame), one must apply the total transformation (T) (35)

$$\begin{bmatrix} x_{co} \\ y_{co} \\ z_{co} \\ 1 \end{bmatrix} = T \begin{bmatrix} X_o' \\ Y_o' \\ Z_o' \\ 1 \end{bmatrix}. \quad (42)$$

2) Case II—Radius is not known: In order to solve this problem, one has to use information from two separate images of a circle. As was discussed earlier, there exist two solutions for the orientation (norm) of a circle. Thus, one must have two

images of the same circle (acquired at two distinct but known positions) in order to determine the unique and acceptable orientation of a circle. As well, one can use the same two images for position determination of the circle. However, the question is "how to move the camera from position 1 to position 2?" in order to be able to solve this problem. In order to simplify the situation, it is proposed to move the camera only along its z axis. It is noted that, for an eye-on-hand system, the transformation between the camera frame and the robot's end-effector frame can be estimated in advance [45]. Furthermore, moving the camera along its optical axis by the robot, generally, involves five degrees of freedom. Thus, the degree of accuracy of this specific motion would be the same as the overall degree of accuracy of the robot for any motion that requires all six degrees of freedom. As a result of this specific choice of camera motion, only the z coordinate of the circle's center would change (with respect to the *camera* frame). It is noted that, by applying the translational transformation (34), the equation of the cone (3) — which is defined initially with respect to the *image* frame — can be obtained with respect to the *camera* frame.

Let the camera displacement h be in the positive direction of the z_c axis. Furthermore, let the initial and final coordinates of the feature's center with respect to the *camera* frame be

$$x_{co1}, \quad x_{co2} = x_{co1}$$
$$y_{co1}, \quad y_{co2} = y_{co1}$$
$$z_{co1}, \quad z_{co2} = z_{co1} - h. \tag{43}$$

Note that the value of h is known (since the extent of the displacement of the camera is under control). Knowing the coefficients of the equation of the plane of a circular feature with respect to the camera frame, (l, m, n), one can estimate the following transformation (T_4) using (19) as:

$$\begin{bmatrix} x_c \\ y_c \\ z_c \\ 1 \end{bmatrix} = \begin{bmatrix} l_1 & m_1 & n_1 & 0 \\ l_2 & m_2 & n_2 & 0 \\ l_3 & m_3 & n_3 & 0 \\ 0 & 0 & 0 & 1 \end{bmatrix} \begin{bmatrix} x'' \\ y'' \\ z'' \\ 1 \end{bmatrix}. \tag{44}$$

This transformation is valid for both camera positions, since the orientation of the camera does not change during relocation. Using (43) and (44), the following relation is obtained:

$$K(z''_{o2} - z''_{o1}) = -h. \tag{45}$$

K is defined at the bottom of this page. Now, if one defines both z''_{o1} and z''_{o2} in terms of r (the unknown radius of the circle), then one can solve (45) and find r, as a result of which the problem reduces to a problem of the kind identified as the first case.

It has been shown that z''_{o1} can be expressed by the following equation (see Appendix B):

$$z''_{o1} = \pm\sqrt{-B'_1/A'_1}\ r \tag{46}$$

where A'_1 and B'_1 have constant values and are defined in terms of the coefficients of the equation of the cone and the elements of the rotational transformation (44). A similar equation can be derived for z''_{o2}

$$z''_{o2} = \pm\sqrt{-B'_2/A'_2}\ r. \tag{47}$$

Using (46) and (47), (45) becomes

$$r = \frac{-h}{K\left[\pm\sqrt{-B'_1/A'_1} \pm \sqrt{-B'_2/A'_2}\right]}. \tag{48}$$

Based on physical conditions, there must be only one acceptable solution for r. Such physical conditions are manifested in the following constraints: the acceptable value of r has to be real and positive, and it must satisfy (45) while z''_{o1} and z''_{o2} have the same sign (see (46) and (47)). These constraints on the four possible solutions of r are sufficient to determine the uniquely acceptable one. Having estimated r, z''_{o1} can be calculated using (46). It is noted that the acceptable solution for z''_{o1} must also satisfy the last constraint mentioned above. Based on the estimated value for z''_{o1}, one can estimate the other two coordinates of the feature's center

$$x''_{o1} = -\frac{B_1 z''_{o1}}{A_1}$$
$$y''_{o1} = -\frac{C_1 z''_{o1}}{A_1} \tag{49}$$

where A_1, B_1, and C_1 have constant values and are defined in terms of the coefficients of the equation of the cone and the elements of the rotational transformation (44); see Appendix B. These are the center coordinates with respect to the $x''y''z''$ frame. Applying the transformation (44), one can get the center coordinates with respect to the $x_c y_c z_c$ frame (the camera frame).

IV. APPLICATION OF THE METHODOLOGY TO 3-D QUADRATIC SURFACES

There exist two possible ways to extend the mathematical method developed above to other 3-D surfaces or 3-D features (as opposed to 2-D features). On the one hand, a problem can be defined as: given a quadratic surface (ellipsoid, paraboloid, hyperboloid, and cylindroid), find the orientation of the plane that intersects the given surface and generates a circular curve. It can be shown that applying the general transformation (15), and following the same procedure formulated in Section III, a set of unique solutions can be obtained for each of the above surfaces. However, since this problem and its solution do not seem to be applicable to the general problem of 3-D object

$$K = \frac{-l_3 m_2 n_1 + l_3 m_1 n_2 + l_2 m_3 n_1 - l_1 m_3 n_2 + l_1 m_2 n_3 - l_2 m_1 n_3}{l_1 m_2 - l_2 m_1}.$$
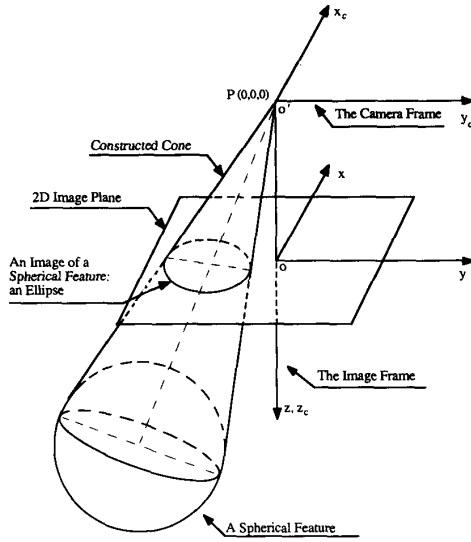
Fig. 3. Schematic representation of the problem for a spherical feature.

recognition, though otherwise having mathematical merit, the details of the solution are not presented here.

On the other hand, a problem can be defined as: given a perspective projection of a 3-D feature (as opposed to a 2-D planar feature that was addressed in the preceding sections), and the effective focal length of the camera, find the feature's location with respect to the camera frame. One such feature of importance in 3-D model-based vision is a spherical feature [40]. Spherical features have also been used for positioning of a mobile robot under a special simplifying condition, namely, that the camera's optical axis passes through the center of the spherical feature [25]. Thus, the problem can be defined more specifically as: given the radius of a sphere, its perspective projection, and the effective focal length of a camera, determine its 3-D position with respect to the camera frame. This problem is shown schematically in Fig. 3.

Let

$$F(x, y, z) \equiv ax^2 + by^2 + cz^2 + 2fyz + 2gzx +$$
$$2hxy + 2ux + 2vy + 2wz + d = 0 \quad (50)$$

be the equation of a quadratic surface. Furthermore, let the equations of the straight lines through a point $P(\alpha, \beta, \gamma)$, whose direction numbers are l_i, m_i, n_i and are tangent to the above quadratic surface, be

$$\frac{x - \alpha}{l_i} = \frac{y - \beta}{m_i} = \frac{z - \gamma}{n_i}. \quad (51)$$

These tangent lines generate a cone that envelopes the quadratic surface. It has been proven [42] that the equation of such an enveloping surface (an enveloping cone) is

$$4F(\alpha, \beta, \gamma)F(x, y, z) =$$
$$\left((x - \alpha)\frac{\partial F}{\partial x} + (y - \beta)\frac{\partial F}{\partial y} + (z - \gamma)\frac{\partial F}{\partial z} + 2F(\alpha, \beta, \gamma) \right)^2. \quad (52)$$

In this equation, the terms $(\partial F/\partial x)$, $(\partial F/\partial y)$, and $(\partial F/\partial z)$ are evaluated at $x = \alpha$, $y = \beta$, and $z = \gamma$.

For the special case under consideration, that for a sphere, the general equation of the surface is defined (with respect to the camera frame) as follows:

$$F(x, y, z) \equiv (x_c - x_o)^2 + (y_c - y_o)^2 + (z_c - z_o)^2 - r^2 = 0. \quad (53)$$

Furthermore, if we consider the origin of the camera frame as the point P, then its coordinates with respect to the camera frame would be $(0, 0, 0)$. Correspondingly, the equation of the enveloping cone (with respect to the camera frame) becomes

$$(x_o^2 + y_o^2 + z_o^2 - r^2)$$
$$\cdot \left((x_c - x_o)^2 + (y_c - y_o)^2 + (z_c - z_o)^2 - r^2 \right)$$
$$= \left(-x_o x_c - y_o y_c - z_o z_c + (x_o^2 + y_o^2 + z_o^2 - r^2) \right)^2. \quad (54)$$

Now, if the camera frame is rotated such that the new z' axis passes through the center of the sphere, then the sphere's center coordinates would be $(0, 0, z_o')$, and the equation of the enveloping cone with respect to the new $x'y'z'$ frame would be (noting that $z_o' > r$)

$$x'^2 + y'^2 - \left(\frac{r^2}{z_o'^2 - r^2} \right) z'^2 = 0. \quad (55)$$

This is the equation of a cone in its central form. Thus, the above-mentioned rotation of the camera frame is the same as the rotational transformation (8). Furthermore, two of the three coefficients in (55) are equal, which corresponds to case IV in Section III-A. As was noted earlier, this case results in a right circular cone, i.e., the principal axis of the cone is perpendicular to its circular base. From a geometrical point of view, this conclusion was expected.

Thus, the analytical solution for the problem would be as follows:

1) Given the effective focal length and the parameters of the perspective projection of a spherical feature — an ellipse — (Fig. 3) with respect to the image frame (the xyz frame), the coefficients of the equation of the constructed cone with respect to the image frame can be obtained using (3). By applying the transformation (34), one can estimate the coefficients of the cone with respect to the *camera* frame.

2) λ_i can be estimated using the parameter values obtained in step 1 and solving (10).

3) Normalizing the first two coefficients of (9) to 1, and equating the third coefficients of (9) and (55), the unknown value z_o' is derived

$$z_o' = \pm \left(\frac{-1 + \lambda_3/\lambda_1}{\lambda_3/\lambda_1} \right)^{1/2} r. \quad (56)$$

The positive solution, being in front of the camera, is the unique acceptable solution for the z_o' coordinate. Thus, the center coordinates with respect to the rotated frame would be $(0, 0, z_o')$.

4) The 3-D coordinates of the center of the spherical feature with respect to the camera frame is determined by applying the rotational transformation (8) to the 3-D coordinates estimated in step 3.

V. EXPERIMENTAL RESULTS

A. Simulated Experimental Results

Three different cases are considered in this section: 1) 3-D orientation and 3-D position estimation of a circular feature when the radius is known, 2) 3-D orientation and 3-D position estimation of a circular feature when the radius is *not* known, and 3) 3-D position estimation of a spherical feature. For each case, first, the simulated experimental setup is presented, and subsequently, the experimental results are given. Finally, the results obtained are compared with the initial setup.

1) Radius Is Known

a) Simulated experimental setup: Let the transformation between the world reference frame and the camera frame be

$$T_w = \begin{bmatrix} x_w \\ y_w \\ z_w \\ 1 \end{bmatrix} = \begin{bmatrix} \frac{\sqrt{3}}{4} & \frac{\sqrt{3}}{2} & \frac{-1}{4} & -10 \\ \frac{3}{4} & \frac{-1}{2} & -\frac{\sqrt{3}}{4} & 10 \\ -\frac{1}{2} & 0 & -\frac{\sqrt{3}}{2} & 30 \\ 0 & 0 & 0 & 1 \end{bmatrix} \begin{bmatrix} x_c \\ y_c \\ z_c \\ 1 \end{bmatrix}$$

and let the equation of a circular feature with respect to the world reference frame be (without loss of generality)

$$x_w^2 + y_w^2 - 16 = 0$$
$$z_w = 0.$$

Then the equation of the cone with the circular feature being its base and its vertex at the center of the camera frame (that is, at the point $(-10, 10, 30)$) would be

$$225x_w^2 + 225y_w^2 + 46z_w^2 - 150y_wz_w$$
$$+150x_wz_w + 240z_w - 3600 = 0.$$

Correspondingly, the equation of the cone with respect to the *camera* frame would be

$$204.024x_c^2 + 225.000y_c^2 + 66.976z_c^2$$
$$-177.452y_cz_c - 127.567z_cx_c - 102.452x_cy_c = 0.$$

Assuming that the *image* plane is at $z_c = +1$ (with respect to the camera frame), then the perspective projection of the circular feature would be (with respect to the image frame xyz)

$$204.024x^2 - 102.452xy + 225.000y^2$$
$$-127.567x - 177.45y + 66.976 = 0.$$

Thus, we can formulate the problem as follows: If the equation of the projection of a circular feature with respect to the *image* frame is given as above, the effective focal length of the camera is 1, and the radius of the feature is 4, then it is required to estimate the surface normal of the feature and subsequently to determine the 3-D position of the feature.

b) Experimental results: First, the parameters of the surface normal are estimated using the computational procedure proposed in Section III-A-3. Subsequently, the 3-D position of the feature is determined using the method proposed in Section III-B-1.

1) The coefficients of the general equation of the cone (with respect to the *image* frame) are

$$a = 204.024$$
$$b = 225.000$$
$$c = 66.976$$
$$2f = -177.452$$
$$2g = -127.567$$
$$2h = -102.452$$
$$2u = -127.567$$
$$2v = 177.452$$
$$2w = 133.952$$
$$d = 66.976.$$

2) Reduction of the equation of the cone leads to

$$\lambda_1 = 274.281$$
$$\lambda_2 = 225.000$$
$$\lambda_3 = -3.281.$$

3) Surface normal parameters are

$$l = \pm 0.421367$$
$$m = 0$$
$$n = 0.906890.$$

As was explained earlier, there exist, in general, two possible solutions. To determine the acceptable one, we must have a second image. In this section we take the *positive* value for l. In Section V-B we will show that this solution is the acceptable solution based on a *second* image.

4) The rotational transformation (see (8)) is

$$T_1 = \begin{bmatrix} -0.413957 & 0.836516 & -0.358998 & 0 \\ 0.875989 & 0.258819 & -0.407009 & 0 \\ -0.247554 & -0.482963 & -0.839919 & 0 \\ 0 & 0 & 0 & 1 \end{bmatrix}.$$

Applying this transformation to the surface's normal vector obtained in step 3 will give us the surface-normal vector with respect to the *camera* frame

$$V_{11} = T_1 \begin{bmatrix} -0.421367 \\ 0 \\ 0.906890 \\ 1 \end{bmatrix} = \begin{bmatrix} -0.5 \\ 0 \\ -0.866025 \\ 1 \end{bmatrix}.$$

Checking the solution: To check the solution obtained, we apply the rotational part of the transformation T_w (R_w) to the vector V_{11}: $V_w = R_wV_{11} = [0011]^t$. This result is what we expected, since the feature's surface normal vector with respect to the world reference frame is $[0011]^t$.

For 3-D position estimation, the estimation process is as follows:

5) Based on the estimated parameters in step 3, the rotational transformation (36) is obtained

$$T_3 = \begin{bmatrix} 0 & -0.906890 & 0.421367 & 0 \\ 1 & 0 & 0 & 0 \\ 0 & 0.4213567 & 0.906890 & 0 \\ 0 & 0 & 0 & 1 \end{bmatrix}.$$

6) Parameters A, B, C, and D are estimated using the elements of the above transformation (T_3) based on (38)

$$A = 225.0$$
$$B = 0$$
$$C = -106.066$$
$$D = 46.0.$$

7) The 3-D position coordinates with respect to the $X'Y'Z'$ frame are estimated using (41)

$$X'_o = 0$$
$$Y'_o = \pm 14.142$$
$$Z'_o = \pm 30.000.$$

8) To obtain the 3-D position of the feature with respect to the *camera* frame, we must apply the total transformation as defined in (35). First, the translational transformation (14), T_2, is estimated using the parameter values obtained in steps 1, 2, and 4:

$$T_2 = \begin{bmatrix} 1 & 0 & 0 & 0.247554 \\ 0 & 1 & 0 & 0.482964 \\ 0 & 0 & 1 & 0.839915 \\ 0 & 0 & 0 & 1 \end{bmatrix}.$$

The transformation between the image frame and the camera frame is

$$T_o = \begin{bmatrix} 1 & 0 & 0 & 0 \\ 0 & 1 & 0 & 0 \\ 0 & 0 & 1 & 1 \\ 0 & 0 & 0 & 1 \end{bmatrix}.$$

Then the total transformation would be

$$T = T_o T_1 T_2 T_3$$
$$= \begin{bmatrix} 0.836516 & 0.224144 & -0.5 & 0 \\ 0.258819 & -0.965926 & 0 & 0 \\ -0.482963 & -0.12941 & -0.866025 & 0 \\ 0 & 0 & 0 & 1 \end{bmatrix}.$$

The 3-D position of the feature with respect to the camera frames is obtained as

$$P_c = T \begin{bmatrix} 0 \\ -14.142 \\ -30.000 \\ 1 \end{bmatrix} = \begin{bmatrix} 11.830 \\ 13.660 \\ 27.811 \\ 1 \end{bmatrix}.$$

Note that we take the *negative* sign for Z'_o in order to get the *positive* value for z_c in the camera frame.

Checking the solution: To check the solution, we estimate the 3-D position with respect to the world reference frame using T_w: $P_w = T_w P_c = [0001]^t$. This is exactly what we expected, since, initially, the feature was placed at (0,0,0) with respect to the world reference frame.

2) Radius Is Not Known

a) Simulated experimental setup: We once more consider the simulated setup in Section V-A as the setup for the *first* camera position and add a simulated setup for the *second* camera position as follows:

Let the transformation between the world reference frame and the camera frame be

$$T'_w = \begin{bmatrix} x_w \\ y_w \\ z_w \\ 1 \end{bmatrix}$$

$$= \begin{bmatrix} \frac{\sqrt{3}}{4} & \frac{\sqrt{3}}{2} & -\frac{1}{4} & -15 \\ \frac{3}{4} & -\frac{1}{2} & -\frac{\sqrt{3}}{4} & 10 - 5\sqrt{3} \\ -\frac{1}{2} & 0 & -\frac{\sqrt{3}}{2} & 30 - 10\sqrt{3} \\ 0 & 0 & 0 & 1 \end{bmatrix} \begin{bmatrix} x'_c \\ y'_c \\ z'_c \\ 1 \end{bmatrix}.$$

This transformation is equivalent to a displacement of the camera frame (from the first camera position to the second camera position) 20 units along the positive direction of the z_c axis of the camera frame.

The equation of the circular feature with respect to the world frame would be the same as before. Then the equation of the cone with the circular feature being its base and its vertex at the center of the camera frame (that is, at the point $(-15, 10 - 5\sqrt{3}, 30 - 10\sqrt{3})$) would be

$$160.770x_w^2 + 160.770y_w^2 + 210.795z_w^2 - 33.975y_w z_w$$
$$+ 380.385z_w x_w + 450.744z_w - 2572.312 = 0$$

and the equation of the cone with respect to the *camera* frame would be

$$103.661x_c'^2 + 160.770y_c'^2 + 267.904z_c'^2$$
$$- 300.000y_c' z_c' - 37.062z_c' x_c' - 173.205x_c' y_c' = 0.$$

Then the perspective projection of the feature (the effective focal length is assumed to be equal to 1) would be (with respect to the image frame xyz)

$$103.661x'^2 - 173.205x'y' + 160.770y'^2$$
$$- 37.062x' - 300.000y' + 267.904 = 0.$$

Thus, we can formulate the problem as follows: If the equations of the two projections of a circular feature with respect to the image frame are given, the effective focal length of the camera is 1 and the displacement of the camera frame along its optical axis is equal to +20, then it is required to estimate the radius and the 3-D orientation and the 3-D position of the feature with respect to the camera frame.

b) Experimental results: Following similar steps as in Section V-A, we would get the following:

1)

$$a = 103.661$$
$$b = 160.770$$
$$c = 267.904$$
$$2f = -300.000$$
$$2g = 37.062$$
$$2h = -173.205$$
$$2u = -37.062$$
$$2v = -300.000$$
$$2w = 535.801$$
$$d = 267.904.$$

2)

$$\lambda_1 = 378.363$$
$$\lambda_2 = 160.770$$
$$\lambda_3 = -6.799.$$

3)

$$l = \pm 0.751624$$
$$m = 0$$
$$n = 0.659592.$$

4)

$$T_1' = \begin{bmatrix} -0.135343 & -0.785548 & 0.603818 & 0 \\ 0.598296 & 0.420974 & 0.681779 & 0 \\ -0.789762 & 0.453536 & 0.413014 & 0 \\ 0 & 0 & 0 & 1 \end{bmatrix}.$$

There exist *two* possible solutions

$$V_{11}' = \begin{bmatrix} 0.296545 \\ 0.899389 \\ -0.321185 \\ 1 \end{bmatrix}$$

$$V_{12}' = \begin{bmatrix} 0.50 \\ 0 \\ 0.866025 \\ 1 \end{bmatrix}.$$

For the first image, the second possible solution is

$$V_{12} = \begin{bmatrix} -0.1511 \\ -0.7382 \\ -0.6574 \\ 1 \end{bmatrix}.$$

Thus, the acceptable surface-normal vector of the feature would be the *common* one, that is

$$V_{11} = V_{12}' = \begin{bmatrix} -0.5 \\ 0 \\ -0.866025 \\ 1 \end{bmatrix}.$$

Note that the above two vectors are equivalent since we are interested in 3-D orientation, not the direction.

5) The transformation (44) would be

$$T_4 = \begin{bmatrix} 0 & 0.866025 & -0.5 & 0 \\ 1 & 0 & 0 & 0 \\ 0 & -0.5 & -0.866025 & 0 \\ 0 & 0 & 0 & 1 \end{bmatrix}.$$

6) The values of the parameters defined in Appendix B are as follows:

First camera position:

$$A_1 = 225.000$$
$$B_1 = 102.452$$
$$C_1 = -27.452$$
$$D_1 = 46.000$$
$$A_1' = 900.000$$
$$B_1' = -50625.000.$$

Second camera position:

$$A_2 = 160.770$$
$$B_2 = 173.205$$
$$C_2 = 80.385$$
$$D_2 = 210.795$$
$$A_2' = 2572.322$$
$$B_{o2}' = -25846.832.$$

7) Based on (48), the two possible (positive) values for the feature's radius are (note that $h = 20$ and $K = -1.154701$)

$$r_1 = 4.000$$
$$r_2 = 1.623.$$

Corresponding to these two values, we can estimate z_{o1}'' and z_{o2}'' using (46) and (47):

$r_1 = 4.000$:

First view: 30.000 and $- 30.000$

Second view: 12.680 and $- 12.680$

$r_2 = 1.623$:

First view: 12.175 and $- 12.175$

Second view: 5.146 and $- 5.146$.

As was indicated in Section III-B-2, the acceptable solution for r must yield values for z_{o1}' and z_{o2}' with the same sign and must satisfy (45). Based on these two constraints, the acceptable solutions for r, z_{o1}'', and z_{o2}'' would be

$$r = 4.000$$
$$z_{o1}'' = -30.000$$
$$z_{o2}'' = -12.680.$$

8) The other two coordinates are (using (49)):

$$x_{o1}'' = 13.660$$
$$y_{o1}'' = -3.660.$$

Applying the rotational transformation (44), (T_4), the 3-D position coordinates with respect to the *camera* frame are obtained:

$$x_{co} = 11.830$$
$$y_{co} = 13.660$$
$$z_{co} = 27.810.$$

Checking the solution: The estimated r is equal to the one initially assumed. As well, the 3-D-position coordinates of the feature are correct, since by applying the transformation T_w, we get $[0, 0, 0, 1]^t$. This is equal to the position vector of the feature with respect to the world reference frame.

3) 3-D Position of a Spherical Feature

a) Simulated experimental setup: Let the 3-D position of the feature be (20,25,30) with respect to the *camera* frame, and let its radius be $r = 5$. Then the equation of the feature would be (using (53))

$$(x_c - 20)^2 + (y_c - 20)^2 + (z_c - 30)^2 - 25 = 0.$$

Furthermore, let the vertex of the enveloping cone be at the origin of the camera frame (0,0,0); Then the equation of the enveloping cone would be (using (54))

$$300x_c^2 + 255y_c^2 + 200z_c^2$$
$$-300y_c z_c - 240z_c x_c - 200x_c y_c = 0.$$

Assuming the image plane is at $z_c = 3$, then the perspective projection of the spherical feature would be (with respect to the image frame xyz)

$$300x^2 - 200xy + 255y^2 - 720x - 900y + 1800 = 0$$
$$z = 0.$$

Thus, we can formulate the problem as follows: If the equation of the projection of a spherical feature with respect to the image frame is given as above, the radius of the feature is equal to 5, and the effective focal length of the camera is equal to 3, then it is required to estimate the 3-D position of the feature.

b) Experimental results: The coefficients of the equation of the cone with respect to the *camera* frame are:

$$a = 300$$
$$b = 225$$
$$c = 200$$
$$2f = -300$$
$$2g = -240$$
$$2h = -200$$
$$2u = 0$$
$$2v = 0$$
$$2w = 0$$
$$d = 0.$$

The coefficients of the central cone equation are obtained using (10)

$$\lambda_1 = 380$$
$$\lambda_2 = 380$$
$$\lambda_3 = -5.$$

Using (56), the feature's 3-D-position with respect to $x'y'z'$ is estimated

$$x'_o = 0$$
$$y'_o = 0$$
$$z'_o = 43.875.$$

The rotational transformation (8) is estimated using (12) and the parameter values obtained in steps 1 and 2

$$T_1 = \begin{bmatrix} 0.427144 & 0.427144 & 0.455842 & 0 \\ 0.533930 & 0.533930 & 0.569803 & 0 \\ -0.729704 & -0.729704 & 0.683763 & 0 \\ 0 & 0 & 0 & 1 \end{bmatrix}.$$

Then the 3-D position coordinates of the spherical feature with respect to the camera frame is obtained as follows:

$$P_c = T_1 \begin{bmatrix} 0 \\ 0 \\ 43.875 \\ 1 \end{bmatrix} = \begin{bmatrix} 20.000 \\ 25.000 \\ 30.000 \\ 1 \end{bmatrix}.$$

The estimated coordinates are correct, since they are equal to the initial 3-D position of the spherical feature with respect to the camera frame.

B. Experimental Results Based on a Real Image

The accurate estimation of the 3-D location of a circular feature from an input grey-level image requires processes to compensate for various types of distortion. In a real process, as opposed to a simulated process, various sources of noise affect the input image and thus distort it. The experimental results in this section report the total process of accurate estimation of the 3-D location of a circular feature, which in part, involves the general 3-D analytical-solution method derived in this paper (without any simplifying assumptions). This section consists of two parts: 1) A brief discussion on a distortion-compensation procedure previously developed and 2) experimental results based on a real image.

1) A Distortion-Compensation Procedure: The details of the various steps required for this purpose, which have already been addressed in other papers (as mentioned below) are not presented here. However, for completeness, a brief review of these steps is presented below:

Camera calibration: The camera is calibrated by applying the mono-view noncoplanar-points technique [16], as a result of which, the 3-D location of the camera frame with respect to a predefined world frame of reference is estimated. Furthermore, the effective focal length of the camera, the radial distortion factor of the camera's lens, and the uncertainty scale factor for the x axis (due to timing mismatches that occur between camera-scanning hardware and image-acquisition hardware) are also obtained.

Subpixel edge detection: After an image of a circular feature is acquired, a new subpixel edge detector is applied [46]. This edge operator is based on the sample-moment-preserving transform (SMPT) and assumes a circular-arc geometry for the boundary inside the detecting area. The result of the edge detector is a set of subpixel edge-point data. The subpixel edge

detector compensates for quantization error and estimates the boundary of a circular feature more reliably.

Coordinate transformation: Computer-image coordinates are expressed in terms of pixel units. To define the edge-points in terms of units of absolute length (in millimeters) and also to compensate for timing mismatches, a set of transformations are applied [16]. These are implemented by using the uncertainty factor estimated in step 1 and technical specifications of the camera's CCD chip and the digitizer board.

Lens-radial-distortion compensation: The estimated lens-radial-distortion factor in step 1 is applied to all edge points to compensate for lens radial distortion [16].

Elliptical-shape-parameters estimation: An interpolation technique based on the optimization of an error function is applied to accurately estimate the five basic parameters of an ellipse — the perspective projection of a circle onto the image plane. It has been shown that, through the application of a newly developed error function, an accurate estimation of elliptical shape parameters can be obtained (even if only an arc of the projected circle is present) [47], [48].

Circular-feature 3-D-orientation estimation: Using the estimated effective focal length in step 1 and the estimated values for the five basic parameters of an ellipse in step 5, and applying the analytical method developed in Section III-A, the orientation of the circular feature with respect to the camera frame is estimated.

Circular-feature 3-D-position estimation: Using the estimated orientation of a circular feature in step 6 and its known radius, and applying the analytical method developed in Section III-B-1, the 3-D position of the feature is estimated with respect to the camera frame. Applying the transformation from the camera frame to the world frame of reference obtained in step 1, to the estimated 3-D position of the circle yields the 3-D position with respect to the world-reference frame.

For a comprehensive explanation of the above sequential distortion-compensation procedure, refer to [49].

2) Experimental Setup: The experimental setup consisted of the following major components: a color video camera: JVC (model TK-870U) with 2/3-in CCD and effective pixels 510H × 492V; a Canon CI-TV lens: 25 mm $f/1.4$; an 8-bit B/W video digitizer: PIP-640B (MATROX Electronic Systems Limited) with 640 × 480 resolution that resided in an IBM-compatible PC-AT; a back-lighting system; an optical table with a gantry-type frame for positioning the camera; and two standard $(x - y)$ translation stages with 40 mm of travel and repeatability better than 2 μm for positioning a calibration plate (thickness: 6 mm) consisting of 30 uniformly spaced (6 × 5) accurately machined through holes (diameter: 25 ± 0.01 mm).

For experimentation on the total process, only 6 of the 30 holes on the calibration plate were used. The selected holes were located on the extreme right and left sides of the calibration plate (i.e., first and last columns of holes). The plate of the circular features, in an inclined orientation with respect to the camera image plane, was positioned such that the field of the selected circles extended over the entire field of view. These conditions provided the most general camera-

TABLE I
ESTIMATED ORIENTATION ANGLES OF THE SURFACE
NORMALS OF A SET OF CIRCULAR FEATURES

Angles	α (degrees)	β (degrees)	γ (degrees)
Reference Angles	89.72	76.73	13.27
Circle 1	88.73	76.06	13.99
Circle 2	89.61	74.99	15.01
Circle 3	88.75	76.54	13.52
Circle 4	89.87	76.39	13.61
Circle 5	89.11	76.43	13.60
Circle 6	87.46	77.93	12.34
Average Angles	88.92	76.39	13.68
Average Deviations	0.80	0.34	0.41

Note: α, β, and γ are the angles that the furface normal of a circle makes with the x, y, and z axes of the camera frame, respectively.

circular-feature configuration. In order to obtain sharp images of all circles, this plate was located within the approximated existing depth of field of the camera [50].

3) Experimental Results for the Total Process: The application of the seven-step procedure (Section V-B-2) to the six coplanar circles resulted in two sets of data, tabulated in Tables I and II. Through camera calibration, the orientation angles of the normal to the circles' plane was estimated. These are referred to as "Reference Angles" in Table I. The estimated orientation angles of each circle's norm are also presented in this table. Note that since the circles were coplanar, they must have the same orientation angles. The average orientation angle is defined as the mean value of the orientation angles of the six circles, while the average deviation is defined as the absolute value of the difference between a reference angle and an average angle. The average deviations for the three orientation angles were determined as, 0.80°, 0.34°, and 0.41°, respectively. As can be seen, the results show only a small error indicative of the good performance of the total process.

In Table II, the results of the position-estimation process are presented. The coordinates, estimated with respect to the world reference frame, are given under the column "Estimated." The exact 3-D coordinates of the circles' centers are known *a priori* and are given in Table II under the column "Reference." The differences between the reference and the estimated coordinates of all the circles are calculated, and the means of these values are given under "Average Deviations." The results can be better appreciated when the size of the field of view (275 mm × 200 mm) and the focused distance (864 mm) are taken into consideration. The 1.28-mm average error for the depth estimation in an approximately 864-mm focused distance is less than 1.5 parts in 1000 average accuracy. As a whole, both sets of results show the validity of the total process involved in the 3-D-location estimation in general, and the applicability of the analytical method developed in this paper in particular.

C. Discussion of Results

We have shown through experimentation that the method developed in this paper works reliably under various camera-

TABLE II
ESTIMATED POSITIONS OF A SET OF CIRCULAR FEATURES

Coordinates	x (mm)		y (mm)		z (mm)	
Circle No.	Reference	Estimated	Reference	Estimated	Reference	Estimated
1	0.00	0.38	0.00	0.63	10.00	8.05
2	185.00	184.78	0.00	-0.03	10.00	11.01
3	0.00	0.24	37.00	37.27	10.00	9.31
4	185.00	184.64	37.00	37.43	10.00	9.15
5	0.00	0.26	74.00	74.34	10.00	8.92
6	0.00	0.46	148.00	148.60	10.00	7.92
Average Deviations	0.32		0.38		1.28	

Note: All the coordinates are with respect to the world reference frame.

feature configurations (three for simulated and six for real experimental setups). However, there exist limitations: From a *mathematical* point of view, the method developed fails when the feature's plane passes through the center of the camera's lens, that is, when the vertex point and the base of the cone are coplanar (this is a *rare* case for a camera-feature configuration). From a *practical* point of view, however, there exists a stronger limitation. In general, the degree of accuracy of the estimated feature's 3-D location depends on how *accurate* we can estimate the parameters of the ellipse — the image of a circular feature — from a grey-level image. Some of the factors involved are addressed in the distortion-compensation procedure mentioned in Section V-B-1. However, there exist two other factors: the size of the feature in the image plane and the relative orientation of the feature plane with respect to the camera image plane (say angle α). The first factor combines the true size of the feature, the distance between the camera and the feature, and the camera's focal length. The second factor concerns the amount of change or deformation of a feature in the image plane with respect to the change of the angle α. For circular features, the ratio of minor to major radii (r and R, respectively) of the ellipse (the image of a circular feature) is roughly equal to $\cos \alpha$. Now, if the difference between the major and minor radii of the ellipse is used as a measure of deformation of a circular feature in the image plane, it would be equal to $R(1 - \cos \alpha)$. Thus, it can be concluded that for small angles α (for example, up to 15°), the amount of deformation is quite small, and as a result it would be very difficult to detect this change from a grey-level image (note that accurate estimation of the ellipse's parameter depends on how accurate the deformation of the ellipse can be detected). This fact can be more appreciated if it is noted that there exists a limit on the accuracy of edge detector operators. As a result, errors in the estimation of 3-D orientation and 3-D position of a feature for small angles α would be more significant. In order to determine the exact limitation of the method from a practical point of view, a complete analysis is required to determine the sensitivity of the parameters of the imaged circular feature in terms of the above-mentioned factors. This is, in fact, a universal problem for all feature-based pose-estimation techniques. Addressing this problem constitutes part of our future work.

VI. CONCLUSIONS

In this paper, the general problem of 3-D location estimation of a circular feature was addressed. This problem has wide applications in machine vision, such as estimation of a mobile robot's location using circular landmarks, for recognition (identification and 3-D location estimation) of 3-D premarked objects using circular markers, for 3-D location estimation of objects that have holes or circular surface contours, for reconstruction of the 3-D structure and motion of a scene undergoing relative rotational motion with respect to the camera, etc. The proposed analytical method is based on decomposition of the 3-D location-estimation problem into two parts: the 3-D orientation estimation of the circular feature and the 3-D position estimation of the feature. For 3-D orientation estimation, a closed-form analytical solution was derived by reducing the general equation of a cone to its central form. For 3-D position estimation of a circular feature, two closed-form solution methods corresponding to two possible cases, whether the radius of the feature is known or not known, were derived. Furthermore, extension of the developed method to 3-D quadratic features (as opposed to 2-D features) was addressed and a closed-form analytical solution method specifically for spherical features was derived. In order to verify the method developed, simulated as well as real experimental setups were employed. Simulated experimental results were obtained for three different cases: 1) 3-D orientation and 3-D position estimation of a circular feature when its radius is known, 2) 3-D position and 3-D orientation estimation of a circular feature when its radius is *not* known, and 3) 3-D position estimation of a spherical feature. The results obtained in all three simulated cases support the analytical method developed in this paper. As well, to demonstrate real experimental results, the method developed was applied to a set of circles located on a calibration plate. The camera was calibrated prior to the application of the method. Also, in order to obtain accurate estimation of the parameters of the imaged circle (that is the corresponding ellipse), a sequential compensation procedure was applied to the input grey-level image. The experimental results obtained for the real case show the validity of the total process involved in the 3-D location estimation of circular features in general, and the applicability of the analytical method developed in this paper in particular.

APPENDIX A
AN ITERATIVE SOLUTION METHOD

Subsequent to application of the rotational transformation (19) to the general equation of conicoids (3) and the plane $lx + my + nz = 0$, the equation of the curve of intersection with respect to the new frame can be derived as

$$[am^2 + bl^2 - 2hlm]x'^2 + [al^2n^2 + bm^2n^2 + c(l^2 + m^2)^2$$
$$+ 2hlmn^2 - 2gln(l^2 + m^2) - 2fmn(l^2 + m^2)]y'^2$$
$$+ [2almn - 2blmn - 2hl^2n + 2hm^2n$$
$$- 2gm(l^2 + m^2) + 2lf(l^2 + m^2)]x'y'$$
$$+ 2[-um\sqrt{l^2 + m^2} + vl\sqrt{l^2 + m^2}]x'$$
$$+ 2[-uln\sqrt{l^2 + m^2} - vmn\sqrt{l^2 + m^2}$$
$$+ w(l^2 + m^2)^{3/2}]y' + (l^2 + m^2)d = 0.$$

The above equation would represent a circle if the following two conditions exist (using conditions (22)):

$$(a - b)lmn + f(l^2 + m^2)l - g(l^2 + m^2)m$$
$$- hl^2n + hm^2n = 0$$
$$am^2 + bl^2 - 2hlm = al^2n^2 + bm^2n^2 + c(l^2 + m^2)^2$$
$$- 2f(l^2 + m^2)mn - 2g(l^2 + m^2)ln$$
$$+ 2hlmn^2.$$

Considering these two equations together with the third equation, $l^2 + m^2 + n^2 = 1$, three nonlinear equations with three unknowns l, m, and n are obtained. From the first equation, n can be expressed in terms of the other two unknowns, based on which, two nonlinear equations (of higher degree) with two unknowns l and m are obtained:

$$am^2 + bl^2 - 2hlm = c(l^2 + m^2)^2 + (al^2 + bm^2 + 2hlm)$$
$$\cdot \left[\frac{-f(l^2 + m^2)l + g(l^2 + m^2)m}{alm - blm - hl^2 + hm^2}\right]^2$$
$$- 2[f(l^2 + m^2)m + g(l^2 + m^2)l]$$
$$\cdot \left[\frac{-f(l^2 + m^2)l + g(l^2 + m^2)m}{alm - blm - hl^2 + hm^2}\right]$$
$$l^2 + m^2 - 1 = -\left[\frac{-f(l^2 + m^2)l + g(l^2 + m^2)m}{alm - blm - hl^2 + hm^2}\right]^2.$$

The variables l and m are of degree eight in the first equation and of degree six in the second equation. Numerical methods must be used to solve these two nonlinear equations. It is apparent that, compared to a closed-form analytical solution method, numerical methods are generally less efficient. Furthermore, the problem of acceptable solutions would remain, since, analytically, these equations can have up to eight sets of solutions, though intuitively it is known that there exist at most two physical solution sets.

APPENDIX B
DERIVATION OF AN EXPRESSION FOR z''_{o1}

Let the equation of the first cone corresponding to the first camera position be (with respect to the *camera* frame)

$$a_1 x_{c1}^2 + b_{c1} y_{c1}^2 + c_1 z_{c1}^2 + 2f_1 y_{c1} z_{c1}$$
$$+ 2g_1 z_{c1} x_{c1} + 2h_1 x_{c1} y_{c1} = 0.$$

Note that since the vertex of the constructed cone is at the origin of the camera frame, the coefficients of x_c, y_c, z_c, and the constant term are all equal to zero. That is, $u = v = w = d = 0$. Applying the transformation (44) to the above equation, the equation of a circle with respect to the $x''_1 y''_1 z''_1$ frame would be obtained. As was shown earlier (see (22)), in the derived equation, the coefficients of x'' and y'' are equal, and the coefficient of the $x''y''$ term is equal to zero. Thus, if

$$A_1 \equiv a_1 l_1^2 + b_1 l_2^2 + c_1 l_3^2 + 2f_1 l_2 l_3 + 2g_1 l_1 l_3 + 2h_1 l_1 l_2$$
$$B_1 \equiv a_1 l_1 n_1 + b_1 l_2 n_2 + c_1 l_3 n_3 + f_1 l_2 n_3 + f_1 l_3 n_2$$
$$+ g_1 l_3 n_1 + g_1 n_3 l_1 + h_1 l_1 n_2 + h_1 l_2 n_1$$
$$C_1 \equiv a_1 m_1 n_1 + b_1 m_2 n_2 + c_1 m_3 n_3 + f_1 m_2 n_3 + f_1 m_3 n_2$$
$$+ g_1 m_3 n_1 + g_1 m_1 n_3 + h_1 m_1 n_2 + h_1 m_2 n_1$$
$$D_1 \equiv a_1 n_1^2 + b_1 n_2^2 + c_1 n_3^2 + 2f_1 n_2 n_3 + 2g_1 n_1 n_3 + 2h_1 n_1 n_2$$

then the equation of the circle becomes (in its standard form)

$$\left[x''_1 + \left(\frac{B_1 z''_1}{A_1}\right)\right]^2 + \left[y''_1 + \left(\frac{C_1 z''_1}{A_1}\right)\right]^2$$
$$= \left(\frac{B_1 z''_1}{A_1}\right)^2 + \left(\frac{C_1 z''_1}{A_1}\right)^2 - \left(\frac{D_1 z''^2_1}{A_1}\right).$$

From the above equation, one can get the radius of a circle in terms of z'_{o1} (where x''_{o1}, y''_{o1}, and z''_{o1} are denoted as the coordinates of the center)

$$\left(\frac{B_1 z''_1}{A_1}\right)^2 + \left(\frac{C_1 z''_1}{A_1}\right)^2 - \left(\frac{D_1 z''^2_1}{A_1}\right) = r^2.$$

Let

$$A'_1 \equiv B_1^2 + C_1^2 - A_1 D_1$$
$$B'_1 \equiv -A_1^2.$$

Then the above equation becomes

$$A'_1 z''^2_{o1} + B'_1 r^2 = 0$$

from which one can derive an explicit expression for z''_{o1}.

REFERENCES

[1] M. A. Fischler and R. C. Bolles, "Random sample consensus: A paradigm for model fitting with applications to image analysis and automated cartography," *Commun. Ass. Comput. Mach.*, vol. 24, no. 6, pp. 381–395, June 1981.
[2] W. J. Wolfe and K. F. Jones, "Camera calibration using the perspective view of a triangle," *SPIE Proc. Automat. Inspection Meas.*, vol. 730, pp. 47–50, Oct. 1986.
[3] S. Linnainmaa, D. Harwood, L. S. and Davis, "Pose determination of a three-dimensional objects using triangle pairs," *IEEE Trans. Pattern Anal. Machine Intell.*, vol. 10, no. 5, pp. 634–647, Sept. 1988.

[4] D. De Menthon and L. S. Davis, "New exact and approximate solutions of the three-point perspective problem," in *Proc. IEEE Int. Conf. Robotics Automat.* (Cincinnati, OH), May 1990, pp. 40–45.

[5] I. Fukui, "TV image processing to determine the position of a robot vehicle," *Pattern Recognit.*, vol. 14, pp. 101–109, 1981.

[6] J. W. Courtney and J. K. Aggarwal, "Robot guidance using computer vision," in *Proc. Trends Applicat.: Automating Intell. Behavior—Applicat. Frontiers* (Gaithersburg, MD), May 1983, pp. 57–62.

[7] Y. Hung, P.-S. Yeh, and D. Harwood, "Passive ranging to known planar point sets," CAR-TR-65, Center for Automat. Res., Univ. of Maryland, College Park, MD, June 1984.

[8] M. M. Trivedi, M. A. Abidi, R. O. Eason, and R. C. Gonzalez, "Object recognition and pose determination in multisensor robotic systems," in *Proc. Int. Conf. Syst. Man Cybern.* (Cambridge, MA), Nov. 1989, pp. 186–193.

[9] R. M. Haralick, "Determining camera parameters from the perspective projection of a rectangle," *Pattern Recognit.*, vol. 22, no. 3, pp. 225–230, 1989.

[10] R. Horaud, B. Conio, and O. Leboulleux, "An analytic solution for the perspective 4-point problem," *Comput. Vision, Graphics Image Processing*, vol. 47, pp. 33–44, 1989.

[11] M. A. Abidi and R. C. Gonzalez, "The use of multisensor data for robotic applications," *IEEE Trans. Robotics Automat.*, vol. 6, no. 2, pp. 159–177, Apr. 1990.

[12] M. A. Abidi and T. Chandra, "Pose estimation for camera calibration and landmark tracking," in *Proc. IEEE Int. Conf. Robotics Automat.* (Cincinnati, OH), May 1990, pp. 420–426.

[13] N.-Y. Chen, J. R. Birk, and R. B. Kelly, "Estimating workpiece pose using the feature points method," *IEEE Trans. Automat. Contr.*, vol. AC-25, no. 6, pp. 1027–1041, Dec. 1980.

[14] T. S. Huang and J. Q. Fang, "Estimating 3-D motion parameters: Some experimental results," in *Proc. SPIE 3rd Int. Conf. Robot Vision Sensory Contr.* (Cambridge, MA), Nov. 1983, pp. 435–437.

[15] S. Ganapathy, "Decomposition of transformation matrices for robot vision," in *Proc. IEEE Int. Conf. Robotics Automat.* (Atlanta, GA), Mar. 1984, pp. 130–139.

[16] R. Y. Tsai, "A versatile camera calibration technique for high-accuracy 3D machine vision metrology using off-the-shelf TV camera and lenses," *IEEE J. Robotics Automat.*, vol. RA-3, no. 4, pp. 323–344, Aug. 1987.

[17] R. M. Haralick and J. Hyonam, "2D-3D pose estimation," in *Proc. IEEE 9th Int. Conf. Pattern Recognit.*, Nov. 1988, pp. 385–391.

[18] L. G. Roberts, "Machine perception of three-dimensional solids," in *Optical and Electro-Optical Information Processing*, J. T. Tippett *et al.*, Eds. Cambridge, MA: MIT Press, 1965, pp. 159–197.

[19] R. M. Haralick, Y. H. Chu, L. T. Watson, and L. G. Shapiro, "Matching wire frame objects from their two dimensional perspective projections," *Pattern Recognit.*, vol. 17, no. 6, pp. 607–619, 1984.

[20] R. M. Haralick, "Solving camera parameters from the perspective projection of a parameterized curve," *Pattern Recognit.*, vol. 17, no. 6, pp. 637–645, 1984.

[21] D. Lowe, "Perceptual organization and visual recognition," Ph.D. dissertation, Stanford Univ., Stanford, CA, Sept. 1984.

[22] L. P. Ray, "Estimation of modeled object pose from monocular images," in *Proc. IEEE Int. Conf. Robotics Automat.* (Cincinnati, OH), May 1990, pp. 408–413.

[23] E. S. McVey and G. L. Jarvis, "Ranking of patterns for use in automation," *IEEE Trans. Ind. Electron. Contr. Instrum.*, vol. IECI-24, no. 2, pp. 211–213, May 1977.

[24] R. A. Young, "Locating industrial parts with subpixel accuracies," *SPIE Proc. Optics, Illumination, Image Sensing Machine Vision*, vol. 728, pp. 2–9, Oct. 1986.

[25] M. J. Magee and J. K. Aggarwal, "Determining the position of a robot using a single calibration object," in *Proc. IEEE Int. Conf. Robotics Automat.* (Atlanta, GA), Mar. 1984, pp. 140–149.

[26] M. R. Kabuka and A. E. Arenas, "Position verification of a mobile robot using standard pattern," *IEEE J. Robotics Automat.*, vol. RA-3, no. 6, pp. 505–516, Dec. 1987.

[27] N. Olgac, Z. Gan, and B. E. Platin, "3-D recognition of object configurations by hybrid projection analysis using a single-camera image," in *Proc. 1st Nat. Appl. Mechanisms Robotics Conf.* (Ohio), Nov. 1989, pp. 1–6.

[28] Y. Fainman, L. Feng, and Y. Koren, "Estimation of absolute spatial position of mobile systems by hybrid opto-electronic processor," in *Proc. IEEE Int. Conf. Syst. Man Cybern.* (Cambridge, MA), Nov. 1989, pp. 651–657.

[29] B. Hussain and M. R. Kabuka, "Real-time system for accurate three-dimensional position determination and verification," *IEEE Trans. Robotics Automat.*, vol. 6, no. 1, pp. 31–43, Feb. 1990.

[30] Z. Zhou, K. C. Smith, B. Benhabib, and R. Safaee-Rad, "Morphological skeleton transforms for determining position and orientation of pre-marked objects," in *Proc. IEEE Pacific Rim Conf. Commun. Computers Signal Process,* (Victoria, BC, Canada), June 1989, pp. 301–305.

[31] R. Safaee-Rad, B. Benhabib, K. C. Smith, and Z. Zhou, "Pre-marking methods for 3D object recognition," in *Proc. IEEE Int. Conf. Syst. Man Cybern.* (Boston), Nov. 1989, pp. 592–595.

[32] D. Wei and M. Gini, "The use of taper light beam for object recognition," in *Robot Vision*, A. Pugh, Ed. London: IFS Publications, 1983, pp. 143–153.

[33] H. C. Lee and K. S. Fu, "3-D shape from contour and selective confirmation," *Comput. Vision, Graphics, Image Processing*, vol. 22, pp. 177–193, 1983.

[34] ——, "Generating object descriptions for model retrieval," *IEEE Trans. Pattern Anal. Machine Intell.*, vol. PAMI-5, no. 5, pp. 462–471, Sept. 1983.

[35] J. W. Bales and L. K. Baker, "Marking parts to aid robot vision," Tech. Paper 1819, NASA, Washington, DC, 1981.

[36] H. S. Sawhney, J. Oliensis, and A. R. Hanson, "Description from image trajectories of rotational motion," in *Proc. 3rd IEEE Int. Conf. Comput. Vision* (Osaka, Japan), Dec. 1990, pp. 494–498.

[37] <mark>R. Safaee-Rad, B. Benhabib, and K. C. Smith,</mark> "Perspective projection and perspective distortion of circular-landmark features," in *Proc. CSECE Canadian Conf. Electrical Comput. Eng.* (Ottowa, ON, Canada), Sept. 1990, pp. 45.3.1–45.3.5.

[38] P. G. Mulgaonkar, "Analysis of perspective line drawings using hypothesis based reasoning," Ph.D. dissertation, Virginia Polytech. Inst. and State Univ., Blacksburg, VA, 1984.

[39] D. H. Marimont, "Inferring spatial structure from feature correspondence," Ph.D. dissertation, Stanford Univ., Stanford, CA, Mar. 1986.

[40] Y. C. Shin and S. Ahmad, "3D location of circular and spherical features by monocular model-based vision," in *Proc. IEEE Int. Conf. Syst. Man Cybern.* (Boston), Nov. 1989, pp. 576–581.

[41] R. Safaee-Rad, K. C. Smith, B. Benhabib, and I. Tchoukanov, "An analytical method for the 3D-location estimation of circular features for an active-vision system," in *Proc. IEEE Int. Conf. Syst. Man Cybern.* (Los Angeles), Nov. 1990, pp. 215–220.

[42] E. Mosnat, *Problemes de Géométrie Analytique*, vol. 3, 3rd ed. Paris: Vuibert, 1921.

[43] R. J. T. Bell, *An Elementary Treatise on Coordinated Geometry of Three Dimensions*, 3rd ed. London: Macmillan, 1944.

[44] B. Nobel and J. W. Daniel, *Applied Linear Algebra.* Englewood Cliffs, NJ: Prentice-Hall, 1977.

[45] Y. C. Shiu, "Calibration of wrist-mounted robotic sensors by solving homogeneous transform equations of the form $AX=XB$," *IEEE Trans. Robotics Automat.*, vol. 5, no. 1, pp. 16–29, Feb. 1989.

[46] I. Tchoukanov, R. Safaee-Rad, B. Benhabib, and K. C. Smith, "Sub-pixel edge detection for accurate estimation of elliptical shape parameters," in *Proc. CSME Mechan. Eng. Forum* (Toronto), June 1990, pp. 313–318.

[47] R. Safaee-Rad, K. C. Smith, and B. Benhabib, "Accurate estimation of elliptical shape parameters from a grey-level image," in *Proc. IEEE Int. Conf. Pattern Recognit.* (Atlantic City, NJ), June 1990, pp. 20–26.

[48] B. B. Chaudhuri, "Optimal circular fit to objects in two and three dimensions," *Pattern Recognit. Lett.*, vol. 11, pp. 571–574, Aug. 1990.

[49] R. Safaee-Rad, I. Tchoukanov, B. Benhabib, and K. C. Smith, "Accurate parameter estimation of quadratic curves from grey-level images," *Comput. Vision, Graphics, Image Process.: Image Understanding*, vol. 54, no. 2, pp. 259–274, Sept. 1991.

[50] R. A. Morton, Ed.,, *Photography for the Scientist*, 2nd ed. London: Academic, 1984.

Reza Safaee-Rad received the B.Sc. degree in applied mathematics from California State University, the B.A.Sc. degree in mechanical engineering from Tehran Polytechnic University, Terhan, Iran, the M.A.Sc. degree in electrical engineering (biomedical field) from the University of Manitoba, Winnepeg, Canada, and the Ph.D. degree in mechanical engineering from the University of Toronto, Toronto, Canada, in 1991.

He has been the Research Director of the Computer Integrated Manufacturing Laboratory at the Department of Mechanical Engineering, University of Toronto, since June 1991. He has published more than 25 papers in the areas of machine vision, computer vision, and biomedical engineering.
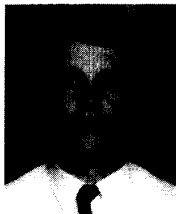
Ivo Tchoukanov (M'91) received the M.Sc. degree in computer science engineering from the Technical University of Sofia, Sofia, Bulgaria.

Since 1989, he has been a Research Associate with the Department of Electrical Engineering at the University of Toronto, Toronto, Canada. His research interests include computer vision, scene understanding, and their application to industry automation and automatic guidance systems.
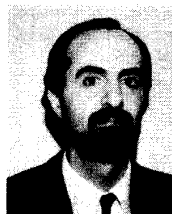
Bensiyon Benhabib is an Associate Professor of Mechanical Engineering and Electrical Engineering at the University of Toronto, Toronto, Canada. His research and teaching interests are in the general area of computer-integrated manufacturing. He has published over 90 scientific and technical papers on subjects such as the analysis and design of robots, robotic sensors, machine vision, workcell management, and production planning.

Dr. Benhabib is a senior member of the SME and a member of the ASME and the CSME.
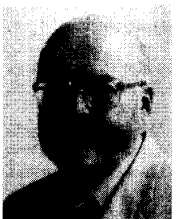
Kenneth Carless Smith (S'53-A'54-M'60-SM'76-F'78) was born in Toronto, Canada, on May 8, 1932. He received the B.A.Sc. degree in engineering physics in 1954, the M.A.Sc. degree in electrical engineering in 1956, and the Ph.D. degree in physics in 1960, all from the University of Toronto, Toronto, Canada.

From 1954 to 1955, he served with Canadian National Telegraphs as a Transmission Engineer. In 1956, he joined the Computation Centre, University of Toronto, as a Research Engineer assigned to assist in the development of high-speed computers at the Digital Computer Laboratory, University of Illinois, Urbana. In 1960, he joined the staff of the Department of Electrical Engineering at the University of Toronto as an Assistant Professor. In 1961, he returned to the University of Illinois as an Assistant Professor of Electrical Engineering where he became Chief Engineer of Illiac II, and then of Illiac III, and attained the rank of Associate Professor of Computer Science. In 1965, he returned to Toronto where he is currently a Professor in the Departments of Electrical Engineering, Mechanical Engineering, Computer Science, and Information Science, and was Chairman of the Department of Electrical Engineering from 1976 to 1981. His research interests include analog, multiple-valued, and binary circuit and systems design, instrumentation in manufacturing, and computer architectures emphasizing parallelism and reliability. He is the coauthor with A. S. Sedra of *Microelectronic Circuits* (HRW/Sauders College Publishing), now in its third edition. He is also an advisor to several international companies in the area of new-product development and education.

Dr. Smith has participated widely in technical and professional organizations, including the IEEE, the Canadian Society for Electrical Engineers (CSEE), and the Canadian Society for Professional Engineers (CSPE). Since 1974, he has served on the Executive Committee of the International Solid-State Circuits Conference as Awards Chairman and in other roles. For the IEEE Computer Society's Technical Committee on Multiple-Valued Logic, he served as Vice-Chair for Technical Activities and Co-Program Chair of ISMVL 92 in Sendai, Japan. He has been President of the CSPE since 1988. He was elected a Fellow of the IEEE in 1978 for his contributions to digital-circuit design.